Electronic Supplementary Material (ESI) for Materials Chemistry Frontiers.

A Novel Lithium-Ion Hybrid Capacitor based on the Aerogel-like MXene Wrapped Fe_2O_3 Nanosphere Anode and the 3D Nitrogen Sulphur Dual-Doped Porous Carbon Cathode

*Xiao Tang [a], Hao Liu [a], Xin Guo [a], Shijian Wang [b], Wenjian Wu [b], Anjon Kumar Mondal [a], Chengyin Wang [c], Guoxiu Wang [a,]**

[a] Centre for Clean Energy Technology, Faculty of Science, University of Technology Sydney, NSW 2007, Sydney, Australia.

[b] Department of Materials Science and Engineering, Dongguan University of Technology, Dongguan, China.

[c] College of Chemistry and Chemical Engineering, Yangzhou University, Yangzhou, China.

Scheme S1. Schematic illustration of the synthesis procedure for the three-dimensional nitrogen sulphur dual-doped porous carbon.

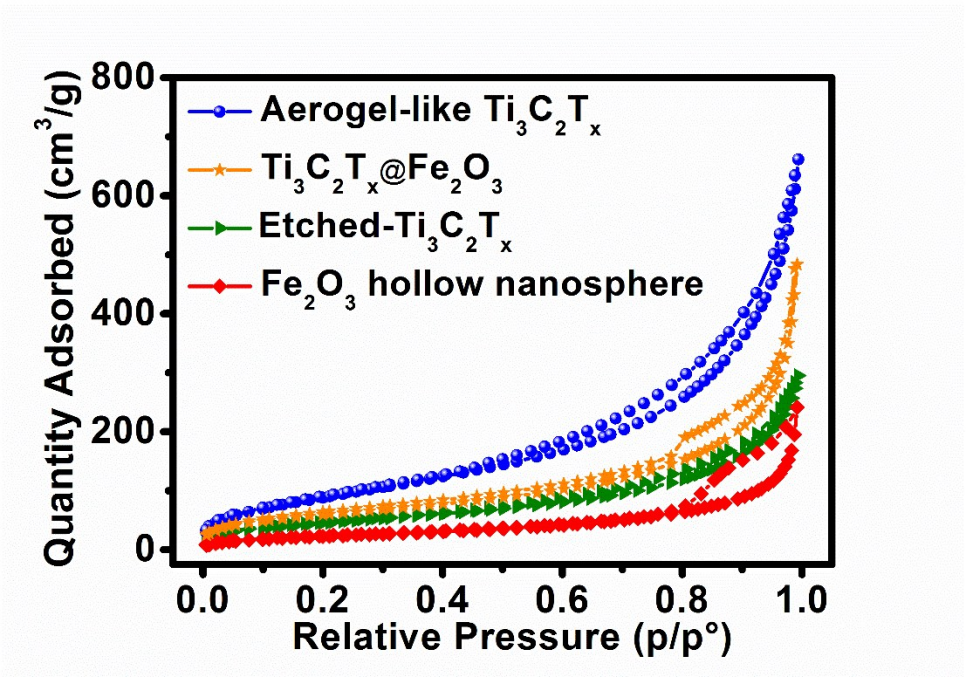

Figure S1. The BET surface area of Aerogel-like $Ti_3C_2T_x$, $Ti_3C_2T_x$@Fe_2O_3, Etched-$Ti_3C_2T_x$ and Fe_2O_3 hollow nanospheres.

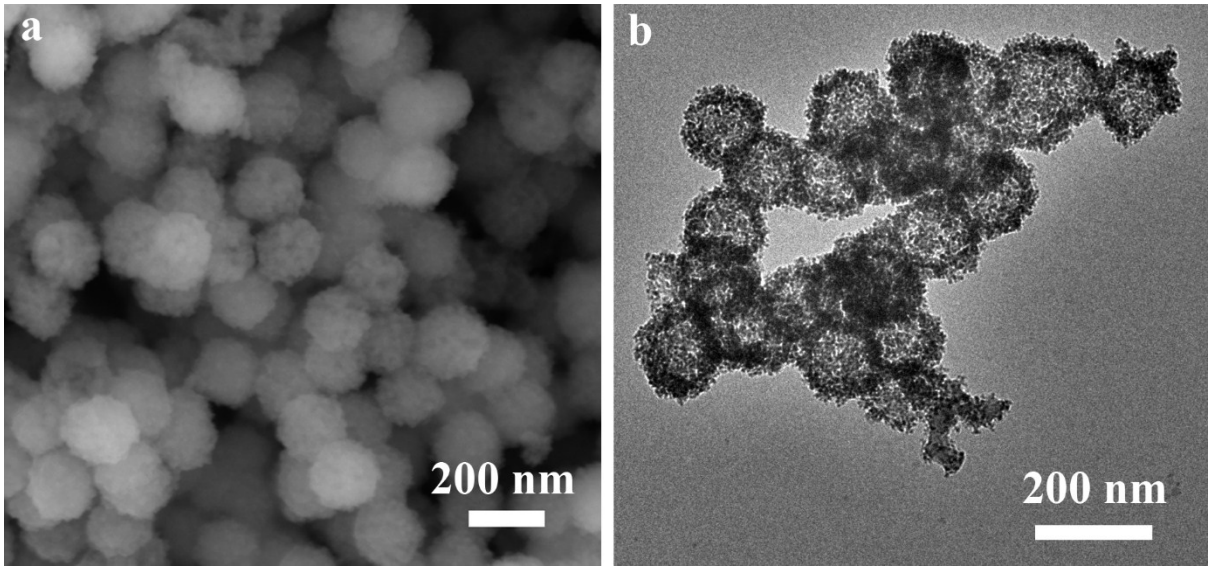

Figure S2. a) SEM image and b) TEM image of Fe_2O_3 hollow nanospheres.

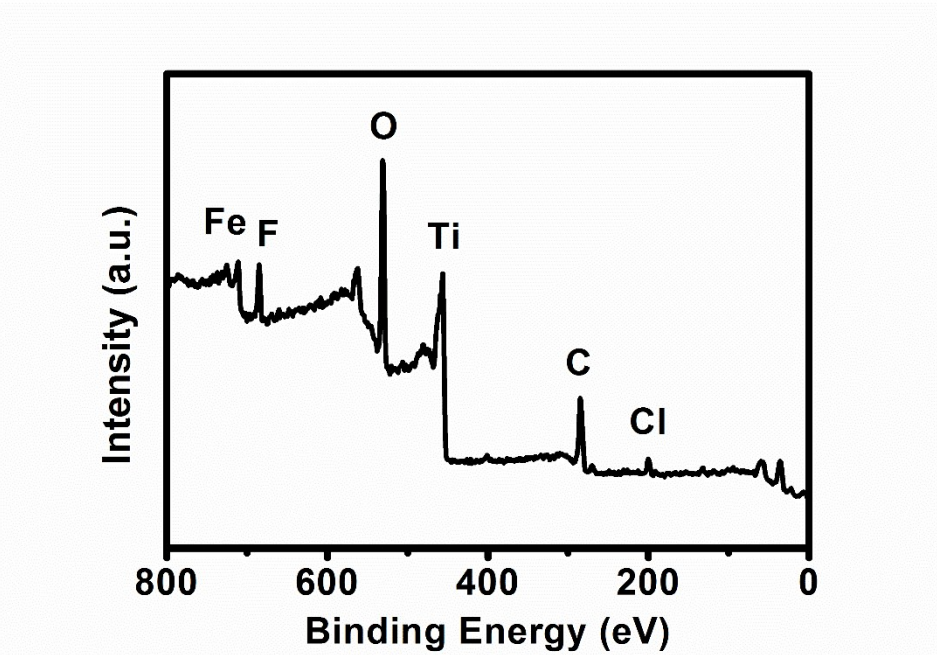

Figure S3. Survey-scan XPS spectrum of $Ti_3C_2T_x$@Fe_2O_3 nanocomposite.

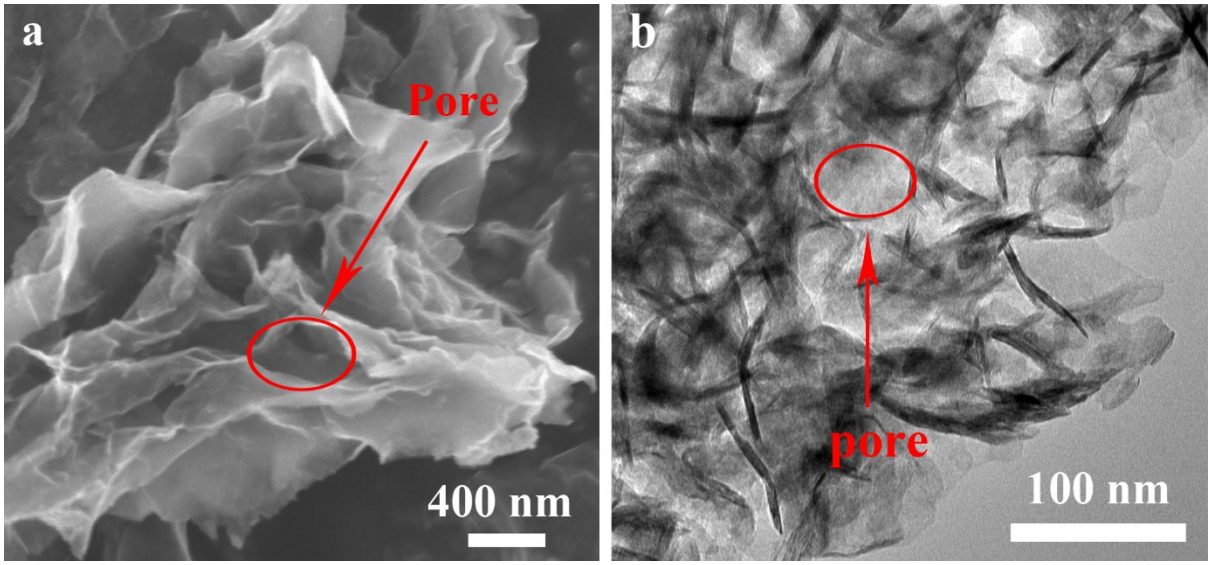

Figure S4. a) SEM image and b) TEM image of the aerogel-like $Ti_3C_2T_x$ MXene.

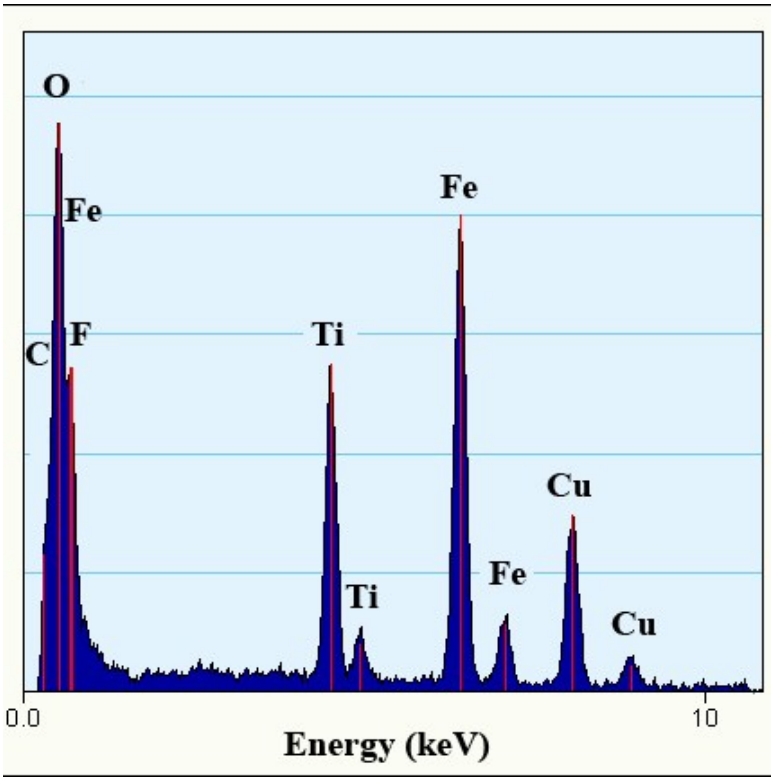

Figure S5. EDS spectrum of the $Ti_3C_2T_x$@Fe_2O_3 composite.

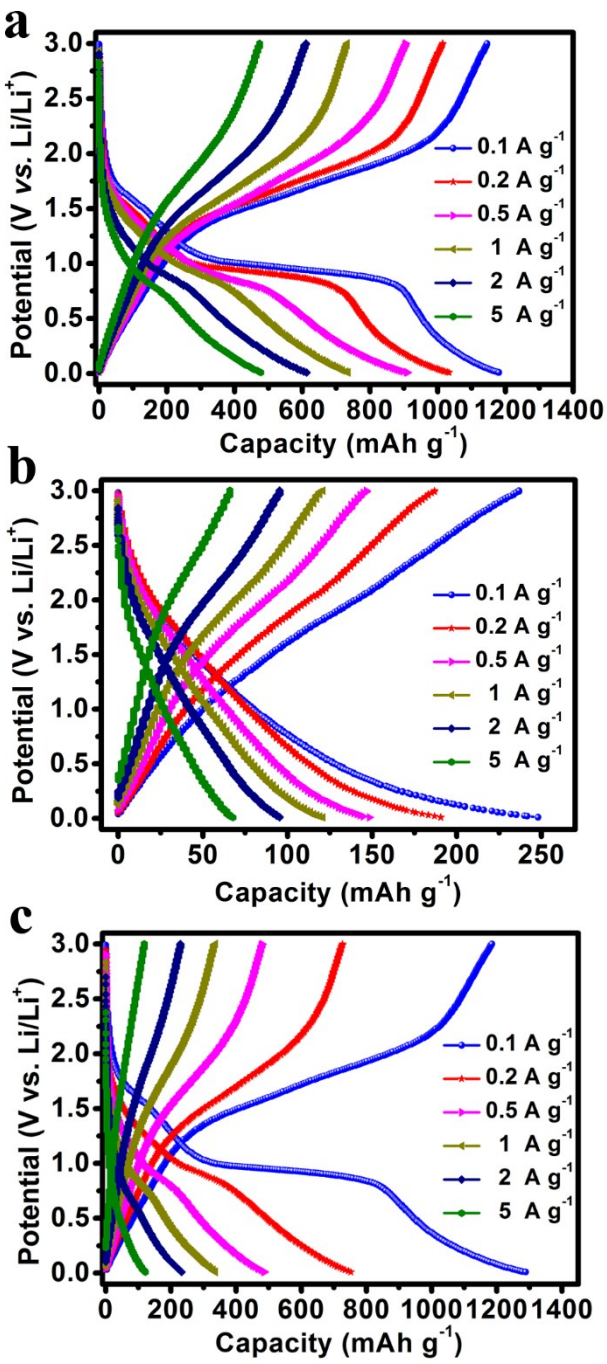

Figure S6. The charge-discharge curves of a) the $Ti_3C_2T_x$@Fe_2O_3 anode, b) the aerogel-like MXene anode and c) the pristine Fe_2O_3 anode at different current density.

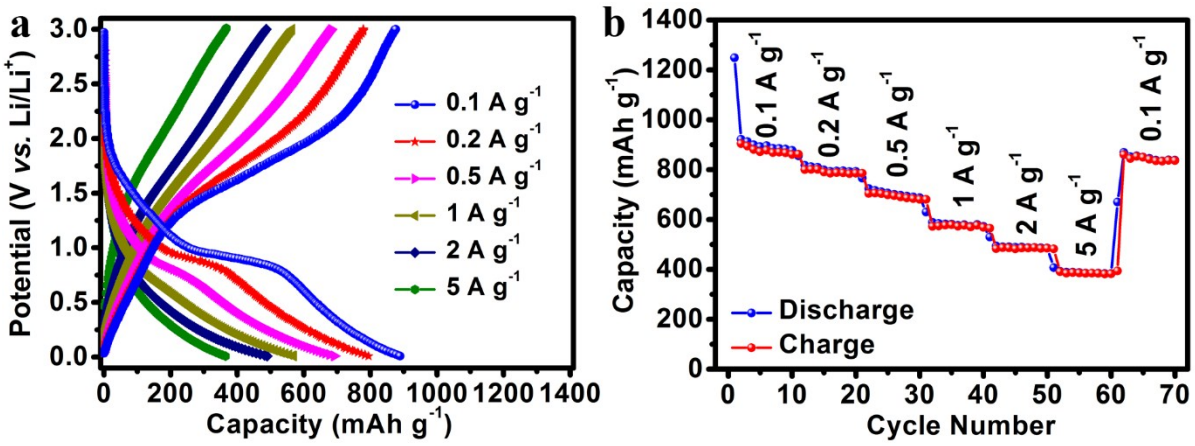

Figure S7. (a) Charge/discharge curves of a $Ti_3C_2T_x$@Fe_2O_3 (1:1) anode at different current densities. (b) Rate performance of the $Ti_3C_2T_x$@Fe_2O_3 (1:1) anode.

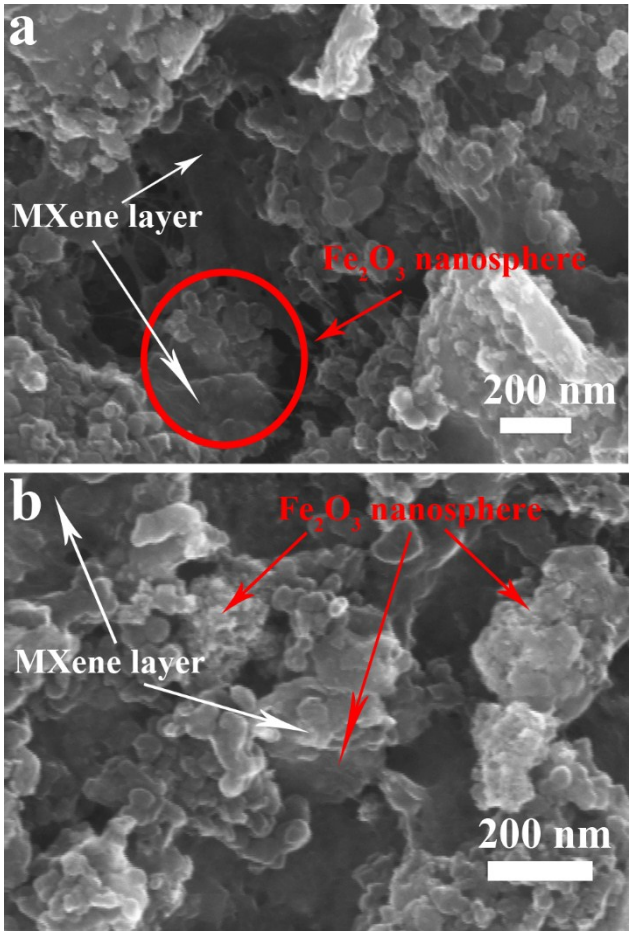

Figure S8. SEM images of $Ti_3C_2T_x$@Fe_2O_3 electrode after 500 cycles.

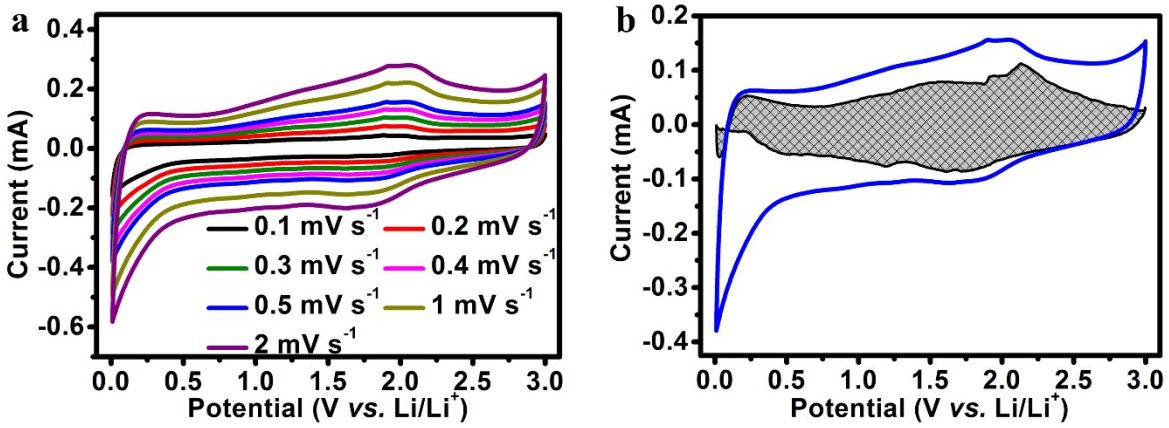

Figure S9. a) The CV curves of the aerogel-like $Ti_3C_2T_x$ MXene anode at different scan rates; b) the capacity separation of the aerogel-like $Ti_3C_2T_x$ MXene anode at the scan rate of 0.5 mV s^{-1}.

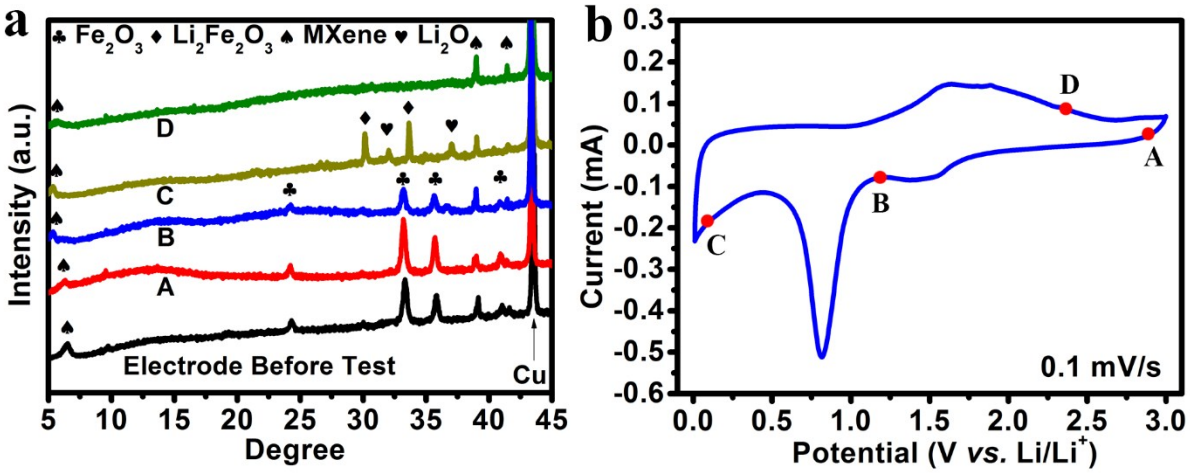

Figure S10. a) *Ex situ* XRD patterns and b) corresponding CV curve collected at a scan rate of 0.1 mV s^{-1} of the hybrid $Ti_3C_2T_x$@Fe_2O_3 electrode.

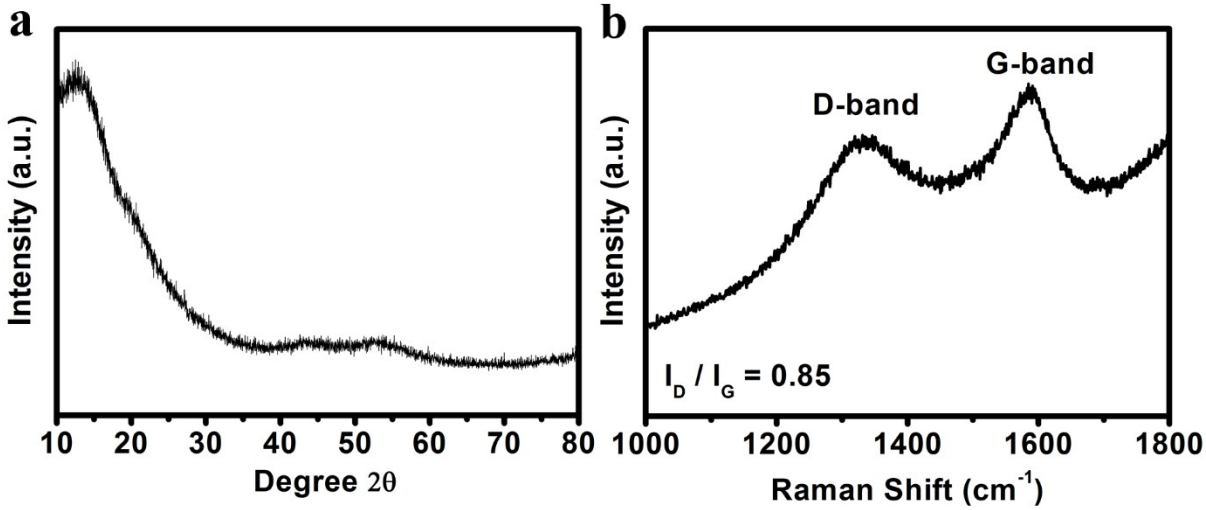

Figure S11. a) XRD pattern and b) Raman spectrum of as-prepared NS-DPC.

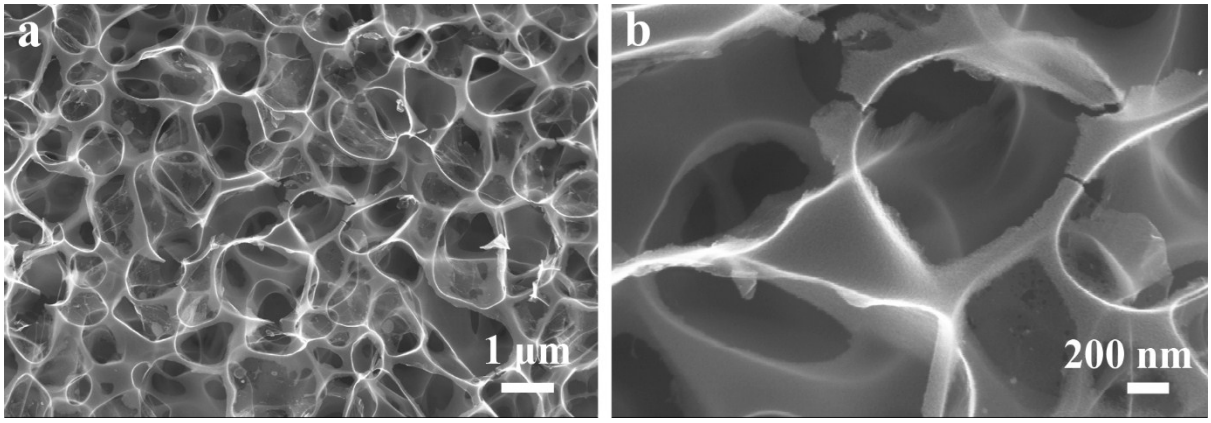

Figure S12. a) Low-resolution SEM and b) high-resolution SEM of nitrogen and sulphur dual-doped porous carbon.

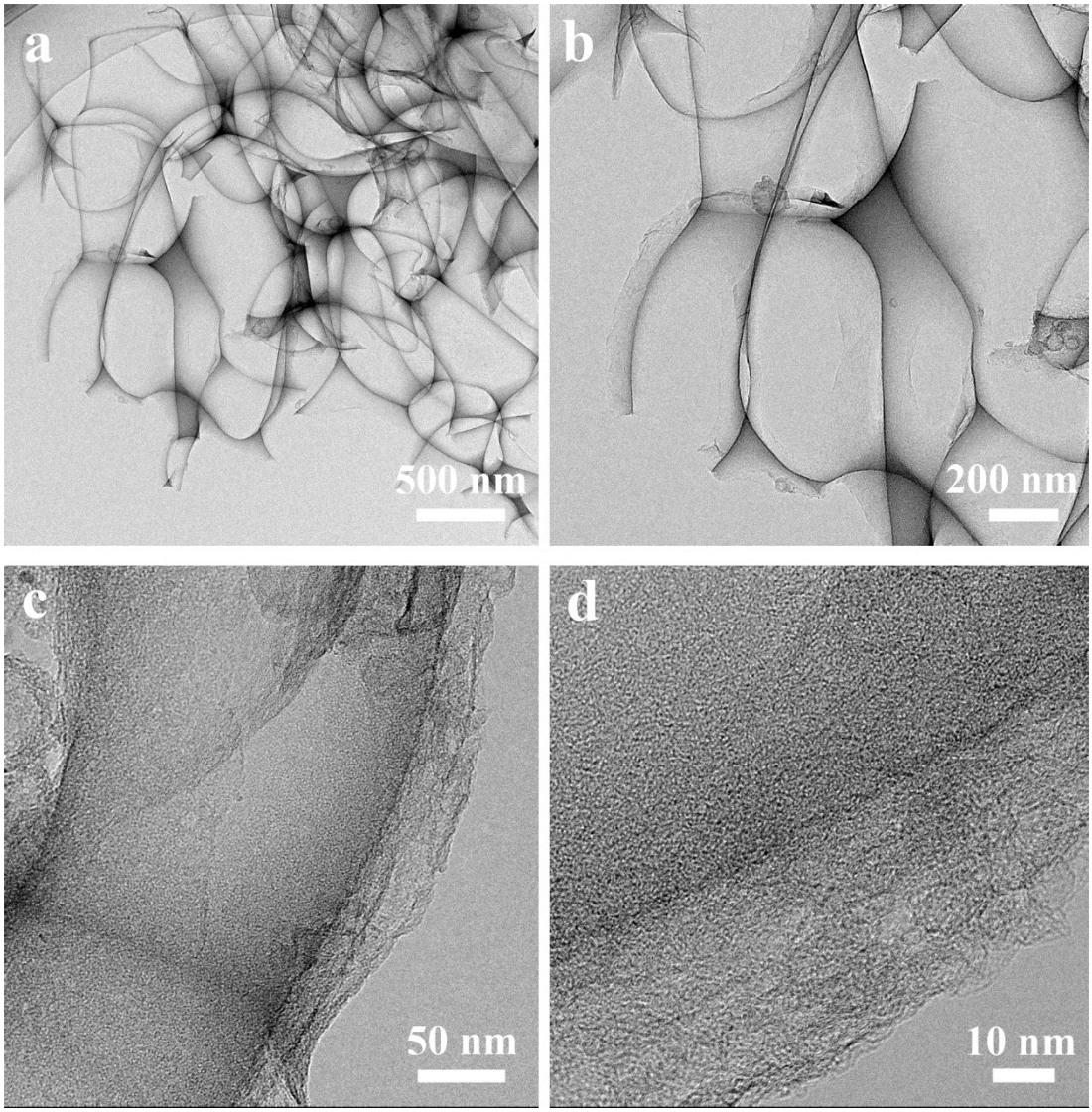

Figure S13. a, b) TEM images and c, d) HRTEM images of NS-DPC.

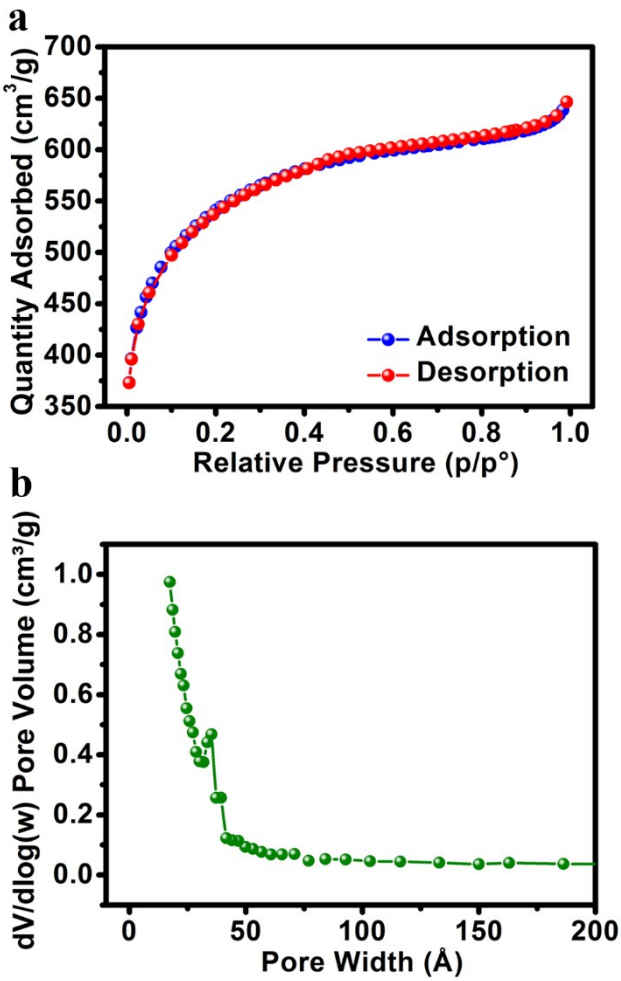

Figure S14. a) The BET surface area of NS-DPC sample. b) Pore size distribution of NS-DPC sample.

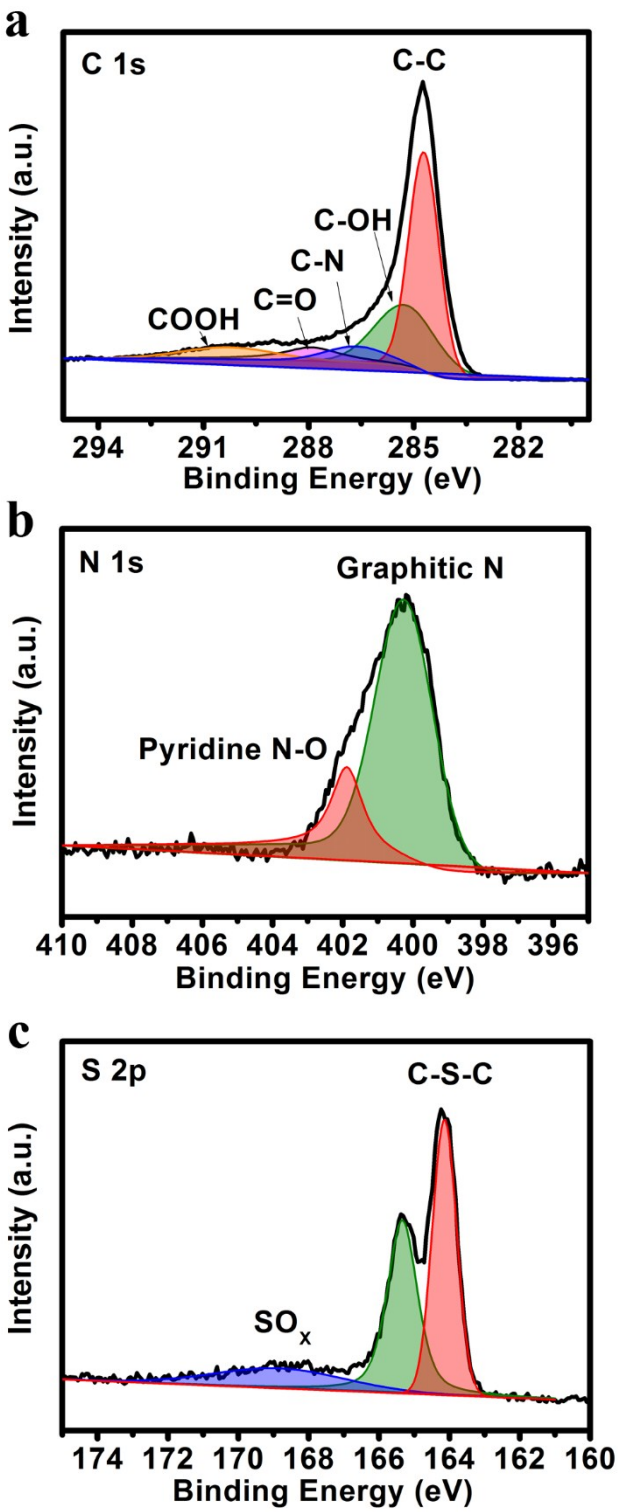

Figure S15. High-resolution a) C 1s, b) N 1s and c) S 2p XPS spectrum of NS-DPC.

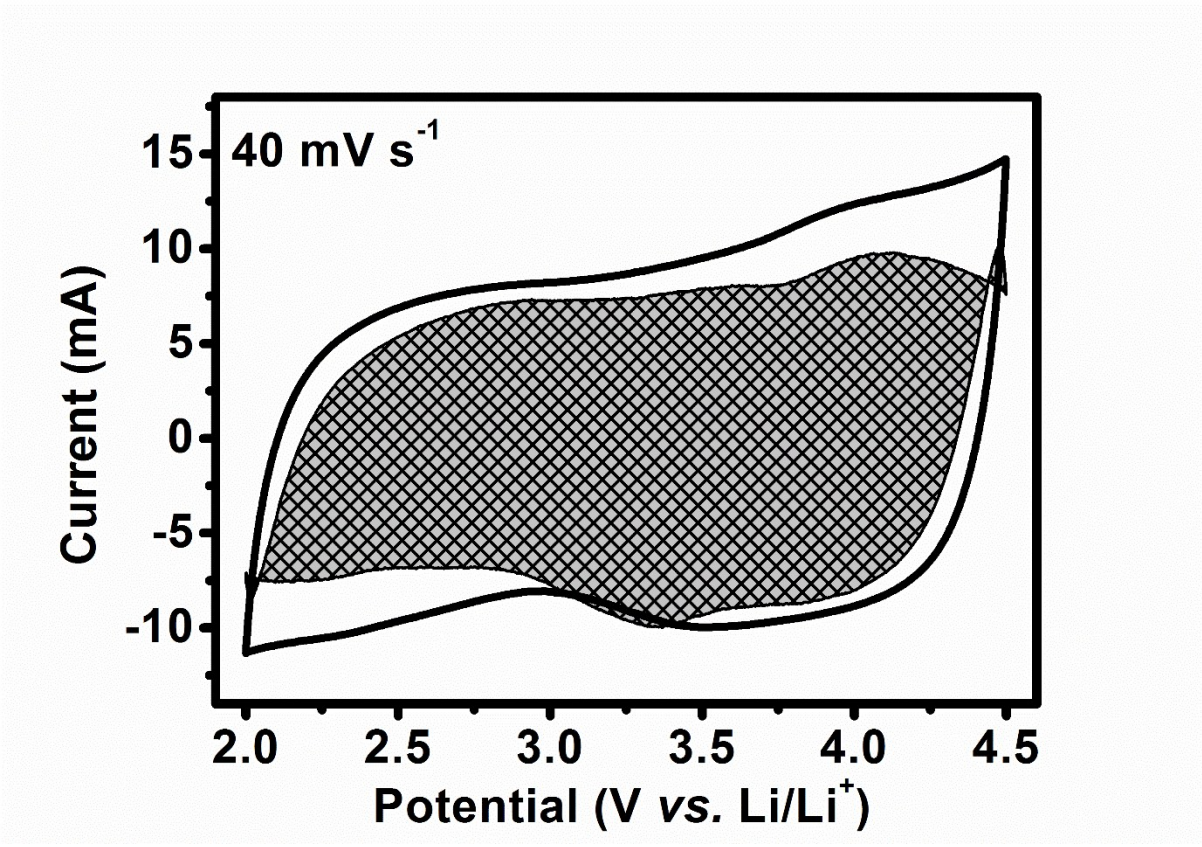

Figure S16. Capacity separation of nitrogen and sulphur dual-doped porous carbon cathode at the scan rate of 40 mV s^{-1}.

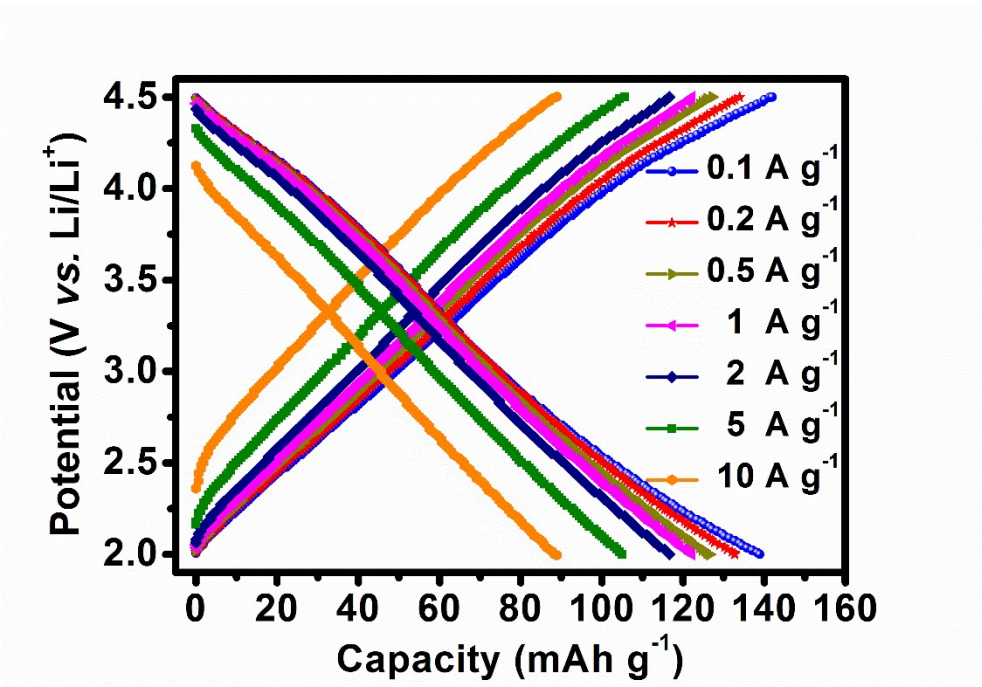

Figure S17. Charge-discharge curves of a NS-DPC cathode tested in $LiPF_6$ electrolyte at different current densities.

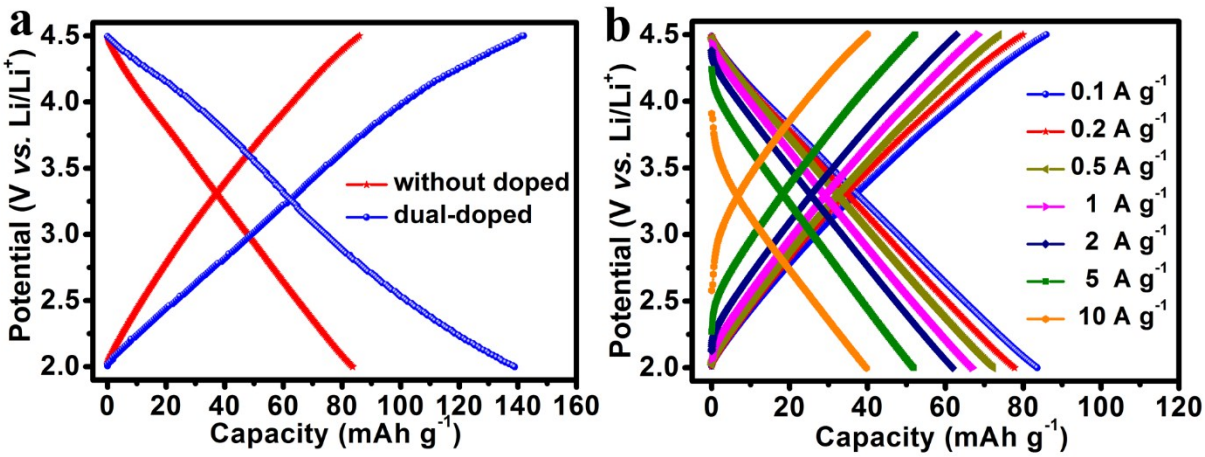

Figure S18. (a) The charge-discharge curves of dual-doped porous carbon cathode and porous carbon cathode without doping (average pore diameter 100 Å ± 10 Å (typical), >99.95% trace metals basis (Aldrich)) at a current density of 0.1 A g^{-1}. (b) The charge-discharge curves of porous carbon without doping at different current densities.

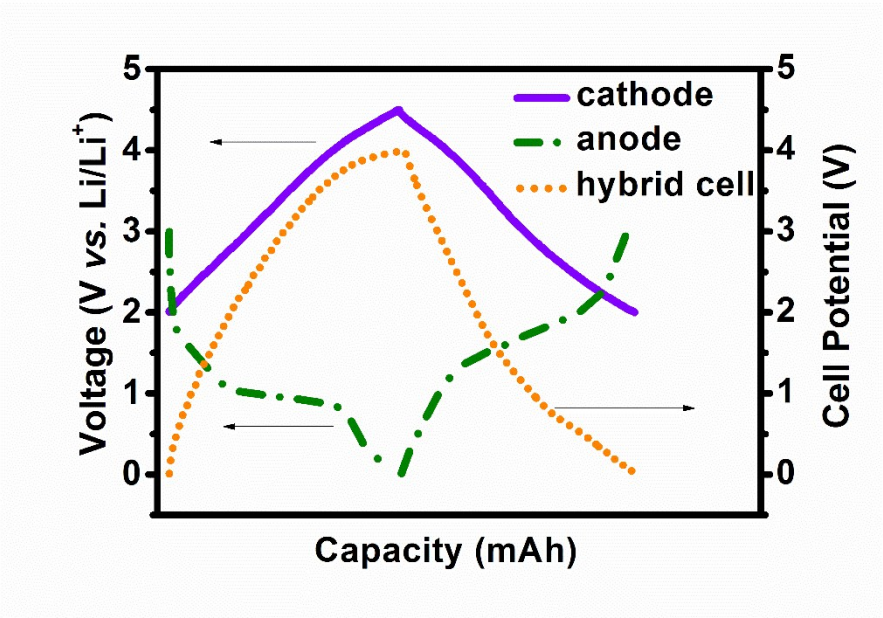

Figure S19. The mechanism of hybrid capacitor to achieve a 4 V potential window.

Table S1. Power and energy densities of $Ti_3C_2T_x@Fe_2O_3$//NS-DPC LIC device obtained at different current density.

Current Desity (A g^{-1})	0.2	0.5	1	2	5	10
Power Density (W kg^{-1})	400	1000	2000	4000	10000	20000
Energy Density (Wh Kg^{-1})	216.16	190.08	168.48	142.56	112.32	96.5

Table S2. Comparison of the electrochemical performances between the $Ti_3C_2T_x$@Fe_2O_3//NS-DPC LIC device and previously reported LICs.

	Voltage Window	Energy Density	Power Density	Cycling Stability	Reference
graphite//AC	1.5-4.5	103.8 Wh kg^{-1}	10 kW kg^{-1}	85%, 10000 cycles	1
hard carbon//AC	2.0-4.2	85.7 Wh kg^{-1}	7.6 kW kg^{-1}	96%, 5000 cycles	2
$Li_4Ti_5O_{12}$/graphene //AC	1-2.5	30 Wh kg^{-1} at 1000 W kg^{-1}	15 kW kg^{-1} at 4 Wh kg^{-1}	84%, 10000 cycles	3
TiO_2// graphene	0.0-3.8	82 Wh kg^{-1} at 570 W kg^{-1}	19 kW kg^{-1} at 21 Wh kg^{-1}	73%, 600 cycles	4
Nb_2O_5/C//AC	1.0-3.5	63 Wh kg^{-1} at 70 W kg^{-1}	16.528 kW kg^{-1} at 5 Wh kg^{-1}	nearly no fading, 1000 cycles	5
Fe_3O_4/Graphene//Graphene	1.0-4.0	147 Wh kg^{-1} at 150 W kg^{-1}	2.587 kW kg^{-1} at 86 Wh kg^{-1}	70%, 1000 cycles	6
MnO/CNS//CNS	1.0-4.0	184 Wh kg^{-1} at 183 W kg^{-1}	15 kW kg^{-1} at 90 Wh kg^{-1}	76%, 5000 cycles	7
VN-RGO//APDC	0.0-4.0	162 Wh kg^{-1} at 200 W kg^{-1}	10 kW kg^{-1} at 64 Wh kg^{-1}	83%, 1000 cycles	8
TiC//PHPNC	0.0-4.5	112 Wh kg^{-1} at 450 W kg^{-1}	67.5 kW kg^{-1} at 35.6 Wh kg^{-1}	83%, 5000 cycles	9
$NiCo_2O_4$//AC	0-4.5	39.4 Wh kg^{-1}	554 W kg^{-1}	no loss, 2000 cycles	10
$Ti_3C_2T_x$@Fe_2O_3//NS-DPC	0.1-4.0	216 Wh kg^{-1} at 400 W kg^{-1}	20 kW kg^{-1} at 96.5 Wh kg^{-1}	87%, 5000 cycles	This work

References:

[1] V. Khomenko, E. Raymundo-Piñero and F. Béguin, *J. Power Sources,* 2008, **177**, 643-651.

[2] J. Zhang, X. Liu, J. Wang, J. Shi and Z. Shi, *Electrochim. Acta,* 2016, **187**, 134-142.

[3] N. Xu, X. Sun, X. Zhang, K. Wang and Y. Ma, *RSC Adv.,* 2015, **5**, 94361-94368.

[4] H. Wang, C. Guan, X. Wang and H. J. Fan, *Small*, 2015, **11**, 1470-1477.

[5] E. Lim, C. Jo, H. Kim, M. H. Kim, Y. Mun, J. Chun, Y. Ye, J. Hwang, K. S. Ha and K. C. Roh, *ACS Nano,* 2015, **9**, 7497-7505.

[6] F. Zhang, T. F. Zhang, X. Yang, L. Zhang, K. Leng, Y. Huang and Y. S. Chen, *Energy Environ. Sci.,* 2013, **6**, 1623-1632.

[7] H. L. Wang, Z. W. Xu, Z. Li, K. Cui, J. Ding, A. Kohandehghan, X. Tan, B. Zahiri, B. C. Olsen, C. M. Holt and D. Mitlin, *Nano Lett.,* 2014, **14**, 1987-1994.

[8] R. T. Wang, J. W. Lang, P. Zhang, Z. Y. Lin and X. B. Yan, *Adv. Funct. Mater.,* 2015, **25**, 2270-2278.

[9] H. W. Wang, Y. Zhang, H. X. Ang, Y. Q. Zhang, H. T. Tan, Y. F. Zhang, Y. Y. Guo, J. B. Franklin, X. L. Wu, M. Srinivasan, H. J. Fan and Q. Y. Yan, *Adv. Funct. Mater.,* 2016, **26**, 3082-3093.

[10] R. Ding, L. Qi and H. Y. Wang, *RSC Adv.,* 2013, **3**, 12581-12584.